

Interaction-dependent anisotropy of fractional quantum Hall states

Akshay Krishna¹, Fan Chen¹, Matteo Ippoliti², and R. N. Bhatt¹

¹*Department of Electrical Engineering and* ²*Department of Physics,*
Princeton University, Princeton NJ 08544, USA

A fractional quantum Hall (FQH) system with broken rotational symmetry exploits its geometric degree of freedom to minimize its ground state energy. The mass anisotropy of bare particles interacting isotropically is partially inherited by the many-body FQH state, and the extent to which it does so depends on the type of interaction, filling fraction and ground state phase. Using numerical infinite density matrix renormalization group simulations, we investigate the transference of elliptical (C_2 -symmetric) anisotropy from the band mass of the bare particles to the FQH states, for various power law interactions. We map out the response of FQH states to small anisotropy as a function of power law exponent, filling, and statistics (bosonic or fermionic) of the constituents. Interestingly, we find a non-analyticity in the linear response of the FQH state at a special filling-dependent value of the power law exponent, above which the interaction effectively becomes zero-range (point-like). We also investigate the effect of C_4 -symmetric band distortions, where we observe a strikingly different dependence on filling.

I. INTRODUCTION

Fractional quantum Hall phases are extreme examples of strongly correlated matter. In a high perpendicular magnetic field, the single-particle spectrum of a two-dimensional electron gas splits into highly degenerate Landau levels separated by cyclotron gaps which may be made arbitrarily large. In this regime, a plethora of interesting phases can be realized^{1,2} as a function of Landau level filling, interaction type and disorder. Some examples are (i) a gapped incompressible fractional quantum Hall (FQH) liquid^{3,4}, (ii) a gapless composite Fermi liquid (CFL)⁵, and translation symmetry-breaking states such as (iii) Wigner crystals⁶ and (iv) charge density waves (CDWs), including stripe and bubble phases⁷.

Following Laughlin's variational wavefunction⁴, the hierarchy⁸ and flux attachment⁹ pictures have paved the way for our understanding of many of the FQH plateaus. This understanding was initially confined to rotationally symmetric Hamiltonians. While it was known that the continuous rotational symmetry was not a necessary ingredient for FQH physics, and that it could be externally broken e.g. by an anisotropic band mass¹⁰, anisotropic FQH states received limited attention until Haldane¹¹ pointed out the presence of an intrinsic geometric degree of freedom of FQH states, acting as a hidden variational parameter in the Laughlin wavefunction. In the past decade, this geometric degree of freedom has received considerable attention¹²⁻³².

Within this framework, theoretical efforts to understand the effects of anisotropy have focussed on anisotropic model wavefunctions^{12,18} and pseudopotentials^{26,27}. These studies have been complemented by computational work on the effects of anisotropy due to band mass, interaction, tilted magnetic fields, and curved space^{13,14,16,19}, as well as the role of filling fraction²⁹. Connecting these results to experiments is not straightforward³³ as gapped states lack a Fermi contour and transport involves anisotropy of scattering as well.

In this work, we study the response of the ground state to anisotropy for various power-law interactions. This provides us with a numerical probe of the 'non-Laughlinness' of the true ground state as the interaction is tuned from Coulomb to shorter ranged. We also investigate the response of FQH states on higher-order anisotropy, i.e. beyond the simplest case of elliptical distortion. This case has not received as much attention, though a few studies exist^{25,34,35}.

In contrast, for gapless fractions like $\nu = 1/2$, the presence of a composite Fermi contour makes direct experimental determination of the effects of Fermi surface deformation feasible³⁶⁻⁴¹. In all cases, the competition between isotropic interaction and an anisotropic bare Fermi contour leads to a measurable effect on the anisotropy of the composite fermion Fermi surface. Numerical calculations²³ agree well with experimental observations; further the extent to which the anisotropy carries over to the composite Fermions depends on the interaction (e.g. its exponent for power-law interactions). It is therefore of interest to see if the dependence of the CFL's response to anisotropy as a function of interaction is qualitatively similar or different to that of gapped FQH states.

Historically, the most popular experimental platforms for the FQH effect have been two-dimensional electron gases confined in semiconductor quantum wells^{3,42-45} and, more recently, graphene⁴⁶⁻⁴⁹. In recent years, there have been efforts to synthesize the FQH states in non-electronic systems, for example using ultracold atoms⁵⁰⁻⁵² and photons^{53,54}. In these systems, interparticle interaction is not expected to be Coulombic, and short range or contact interactions are typically assumed. These are compelling motivations for us to study the interplay of anisotropy and interaction for both fermionic and bosonic quantum Hall fractions.

The effect of anisotropy of the Hamiltonian will depend on the Landau level in question. Higher Landau levels are known to be more prone to instabilities towards rotational and translational symmetry breaking phases. The problem of anisotropy-induced phase transi-

tions in $n > 0$ Landau levels has received much attention both from theory^{32,55,56} and from experiment^{57–60} and holds many interesting open questions. In this paper, however, we focus on incompressible FQH states in the lowest ($n = 0$) Landau level (LLL) that are stable to the application of anisotropy, and study their linear response to weak distortions that are far from any instability. For strong enough distortions, we generally expect every FQH state to transition into a symmetry-broken phase. Characterizing this transition and its dependence on filling and interaction type is left to future work.

This paper is organized as follows. In Section II, we describe the Hamiltonian of our system and sketch the computational method underlying our calculations. In Section III, we provide a theoretical analysis of what should be expected in the case of fermionic FQH states, and present numerical results which are in agreement with those expectations. Section IV describes our exploration of corresponding bosonic FQH states. In Section V, we present our results for C_4 symmetric distortions in the $\nu = 1/3$ and $1/5$ fermionic FQH states. We conclude in Section VI with a discussion of our results.

II. MODEL AND METHOD

Our system is described by the usual quantum Hall Hamiltonian for N_e electrons in perpendicular magnetic field $\mathbf{B} = B\hat{\mathbf{z}}$, and corresponding magnetic vector potential \mathbf{A} :

$$\begin{aligned} H &= \sum_{i=1}^{N_e} T_i + H_{\text{int}} \\ &= \frac{1}{2} \sum_{i=1}^{N_e} (m^{-1})^{ab} \pi_{i,a} \pi_{i,b} + \frac{1}{2} \sum_{i \neq j}^{N_e} V(\mathbf{r}_i - \mathbf{r}_j). \end{aligned} \quad (1)$$

The first term above is the kinetic energy, defined in terms of the dynamical momentum of the i^{th} electron $\boldsymbol{\pi}_i = \mathbf{p}_i - e\mathbf{A}_i$. The inverse mass tensor is denoted m^{-1} . Summation over the spatial indices $a, b \in \{x, y\}$ is implicit.

The second term in Eq. (1) is the interaction potential H_{int} , which we take to be of the form $V(\mathbf{r}) \equiv V(|\mathbf{r}|_\varepsilon)$. The distance $|\mathbf{r}|_\varepsilon$ depends on the dielectric tensor ε , which defines a spatially uniform metric $|\mathbf{r}|_\varepsilon^2 \equiv \varepsilon_{ab} r^a r^b$. The two metrics described by m_{ab} and ε_{ab} are independent. A linear change of coordinates can get rid of the anisotropy in either one of them, but not both simultaneously. Without loss of generality, we take the interaction to be isotropic, $\varepsilon = \mathbf{1}$, which is accomplished by applying the linear transformation $\varepsilon^{-1/2}$ to the coordinates. We can then rotate coordinates to make the mass tensor diagonal, though not proportional to the identity: $m_{ab} = \text{diag}(m_{xx}, m_{yy})$, $m_{xx} \neq m_{yy}$. The single particle

kinetic energy T_i of Eq. (1) then becomes

$$T_i = \frac{\pi_{i,x}^2}{2m_{xx}} + \frac{\pi_{i,y}^2}{2m_{yy}}. \quad (2)$$

We define $\alpha \equiv \sqrt{m_{yy}/m_{xx}}$ as the anisotropy of the non-interacting system.

We refer to this type of anisotropy, which is invariant under C_2 discrete rotational symmetry, as elliptical or two-fold anisotropy²⁵. The first part of the present work analyzes this case. In Sec. V, we consider a generalization of the kinetic energy term of Eq. (1) to non-quadratic functions $T_i(\boldsymbol{\pi}_i)$ whose equal-energy contours are not ellipses. Such a description allows us to study N -fold anisotropy ($N > 2$), as may arise naturally from the symmetries of crystalline band structures.

In the limit of high magnetic field B , the cyclotron energy ω_c is much larger than other energy scales in the problem, and we may safely project all the dynamics to the lowest Landau level (LLL). In this limit, mixing with higher Landau levels is negligible. The kinetic energy of the system is thus quenched, and the Hamiltonian reduces to

$$H_{\text{LLL}} = \frac{1}{2} \sum_{i \neq j}^{N_e} \sum_{\mathbf{q}} V(\mathbf{q}) |F_0(\mathbf{q})|^2 e^{i\mathbf{q} \cdot (\mathbf{R}_i - \mathbf{R}_j)}, \quad (3)$$

where $\mathbf{R}_i \equiv \mathbf{r}_i - \frac{l_B^2}{\hbar} \boldsymbol{\pi}_i \times \hat{\mathbf{z}}$ is the guiding center operator of the i^{th} electron and $V(\mathbf{q})$ is the Fourier transform of the interaction potential $V(\mathbf{r})$. The form factor $F_0(\mathbf{q})$ accounts for the projection of the potential into the basis of anisotropic LLL orbitals, and encodes their anisotropy:

$$|F_0(\mathbf{q})|^2 = \exp \left[-\frac{l_B^2}{2} \left(\alpha q_x^2 + \frac{q_y^2}{\alpha} \right) \right]. \quad (4)$$

We seek to compute the anisotropy of the many-body quantum Hall ground state, denoted by α_{QH} . This is facilitated by introducing a different parametrization of the anisotropies α and α_{QH} , following Ref.²⁹. Since a $\pi/2$ rotation maps $\alpha \mapsto 1/\alpha$ and $\alpha_{\text{QH}} \mapsto 1/\alpha_{\text{QH}}$, in the 2D thermodynamic limit one has the reciprocity relation

$$\alpha_{\text{QH}}(1/\alpha) = \frac{1}{\alpha_{\text{QH}}(\alpha)}. \quad (5)$$

In terms of the logarithmic quantities

$$\gamma \equiv \ln \alpha \quad \text{and} \quad \sigma \equiv \ln \alpha_{\text{QH}}, \quad (6)$$

Eq. (5) becomes

$$\sigma(-\gamma) = -\sigma(\gamma). \quad (7)$$

For small anisotropy, one can expand around the isotropic point $\gamma = \sigma = 0$ and obtain

$$\sigma(\gamma) \approx c_1 \gamma + \mathcal{O}(\gamma^3). \quad (8)$$

The quadratic coefficient is automatically absent due to symmetry, and the linear coefficient $0 \leq c_1 \leq 1$ quantifies the extent to which the band mass anisotropy is transferred to the quantum Hall state, with deviations $\mathcal{O}(\gamma^3)$.

For our numerical calculations, we set up the system on an infinite cylinder, with axis along $\hat{\mathbf{x}}$ and circumference L_y . Combined with the choice of Landau gauge $\mathbf{A} = Bx\hat{\mathbf{y}}$, this allows us to map the problem to a one-dimensional fermion chain and take advantage of the matrix-product states formalism. We use the infinite Density Matrix Renormalization Group (iDMRG) algorithm for quantum Hall states^{61,62}. This introduces a second cut-off in the problem, besides L_y : the bond dimension χ , i.e. the maximum dimension of the matrices used to approximate the many-body ground state. After converging to the approximate ground state for a given anisotropy γ and circumference L_y , we calculate the guiding center structure factor $S(\mathbf{q})$, defined below. The effect of anisotropy is quantified by the long wavelength behavior of $S(\mathbf{q})$ (for gapped FQH states), or the non-analyticities of $S(\mathbf{q})$ at the composite fermion surface (for gapless CFL states). We briefly review the procedure by which the anisotropy is calculated from $S(\mathbf{q})$ below. A detailed discussion may be found in Ref.²⁹.

The guiding center structure factor $S(\mathbf{q})$ is defined as

$$S(\mathbf{q}) = \frac{1}{N_\phi} \langle \delta\rho(\mathbf{q})\delta\rho(-\mathbf{q}) \rangle, \quad (9)$$

where $\delta\rho(\mathbf{q}) \equiv \rho(\mathbf{q}) - \langle \rho(\mathbf{q}) \rangle$ and

$$\rho(\mathbf{q}) = \sum_{j=1}^{N_e} e^{i\mathbf{q}\cdot\mathbf{R}_j} \quad (10)$$

is the Fourier transform of the guiding center density operator. Due to the incompressibility of gapped FQH states, the structure factor is quartic at long wavelengths^{63,64}. Since our simulations are on an infinite cylinder, we have access to a continuum of wavevectors q_x , and may express the long-wavelength structure factor

$$S(q_x, 0) \approx \lambda(\gamma)q_x^4 \quad \text{as} \quad q_x \rightarrow 0. \quad (11)$$

The prefactor $\lambda(\gamma)$ is obtained numerically by taking the limit

$$\lambda(\gamma) = \lim_{q_x \rightarrow 0} S(q_x, 0)/q_x^4. \quad (12)$$

The dependence of this prefactor on γ may be split into even and odd parts as $\lambda(\gamma) = e^{2(D(\gamma)+\sigma(\gamma))}$. The even term $D(\gamma)$ represents an isotropic rescaling of the structure factor, and was found in Ref.²⁹ to be nearly constant in Laughlin fractions with Coulomb interaction. The term we are interested in is $\sigma(\gamma)$, which flips sign when we rotate the anisotropy by an angle of $\pi/2$ (i.e. transform $\gamma \rightarrow -\gamma$). This is the term that controls the ellipticity of contours of $S(\mathbf{q})$ and is a useful proxy for the anisotropy

of the many-body ground state wavefunction itself. It is calculated as

$$\sigma(\gamma) = \frac{1}{4} \ln \frac{\lambda(\gamma)}{\lambda(-\gamma)}. \quad (13)$$

We sweep over a range of anisotropies $-0.3 < \gamma < 0.3$ ($0.74 < \alpha < 1.35$) to obtain a linear fit $\sigma(\gamma) \simeq c_1\gamma$.

For the gapless state at $\nu = 1/2$, the structure factor $S(\mathbf{q})$ has singularities at \mathbf{q} values corresponding to scattering processes between different points on the composite Fermi surface of the CFL. As described in Refs.^{23,65}, placing the system on an infinite cylinder discretizes the momentum in the $\hat{\mathbf{y}}$ direction, $q_y \in (2\pi/L_y)\mathbb{Z}$, so that the Fermi contour consists of isolated points. Sharp features in $S(q_x, q_y)$ allow us to pinpoint the coordinates of these points. By aggregating data from multiple values of the circumference L_y , we can gather enough points to accurately reconstruct the elliptical shape of the two-dimensional Fermi contour and extract its anisotropy.

Capturing the behavior of the system in the thermodynamic limit from finite size iDMRG calculations requires care. The circumference of the cylinder L_y must be large enough to avoid spurious effects from periodic boundary conditions along that direction. However, the entanglement entropy S across a constant- x cut in the cylinder obeys an area law, and thus grows linearly in L_y . The bond dimension χ required to capture this entanglement accurately increases *exponentially*: $\ln \chi \gtrsim S \sim L_y$. Since the computational complexity of iDMRG is at least $\mathcal{O}(\chi^4)$, we are limited to a range of circumferences $14l_B \leq L_y \leq 30l_B$, for which bond dimensions $\chi \leq 4096$ provide accurate results.

The only form of the interaction $V(r)$ for which the analytical expression of $\sigma(\gamma)$ is known is that of a Gaussian interaction with characteristic length sl_B , i.e. $V(r) = e^{-\frac{1}{2}(r/sl_B)^2}$, due to Yang⁶⁶. Since the form factor of the LLL is also a Gaussian, a clever rearrangement of terms provides a closed-form expression for the anisotropy of the quantum Hall state:

$$\begin{aligned} \sigma(\gamma) &= \frac{1}{2} \ln \left(\frac{e^\gamma + s^2}{e^{-\gamma} + s^2} \right) \\ &= \frac{1}{s^2 + 1} \gamma + \frac{s^2(s^2 - 1)}{6(s^2 + 1)^3} \gamma^3 + \dots \end{aligned} \quad (14)$$

The linear coefficient $c_1 = \frac{1}{s^2 + 1}$ decreases as the range s of the isotropic interaction is made larger.

For power law interactions, which we consider here, there is no simple expression for c_1 , and we must compute it numerically as described in the following sections.

III. FERMIONIC STATES

Any interaction $V(\mathbf{r})$ can be expanded in terms of its Haldane pseudopotentials V_m in the lowest Landau level.

In terms of these pseudopotentials, the ground state energy E_{gs} of a configuration of N_e electrons with many-body wavefunction $|\psi\rangle$ is

$$E_{\text{gs}} = \langle \psi | H_{\text{LLL}} | \psi \rangle / \langle \psi | \psi \rangle = \binom{N_e}{2} \sum_{n=0}^{\infty} A_{2n+1} V_{2n+1}. \quad (15)$$

Here $A_n \geq 0$ is the probability for two electrons to have relative angular momentum $n\hbar$, and $\sum_n A_n = 1$. Antisymmetry ensures that any valid fermionic ground state wavefunction $|\psi\rangle$ has all even A_n equal to zero.

The Laughlin wavefunction at filling $\nu = 1/m$ is

$$\psi_L^{(m)}(\mathbf{r}_1, \dots, \mathbf{r}_{N_e}) = \prod_{i>j} (z_i - z_j)^m \exp\left(-\sum_{i=1}^{N_e} \frac{|z_i|^2}{4l_B^2}\right), \quad (16)$$

where $z_j = (x_j - iy_j)/l_B$ is the complex valued position of the j^{th} electron. This wavefunction has the additional feature that odd coefficients A_n vanish for all $n < m$. By Eq. (15), the Laughlin state $|\psi_L^{(m)}\rangle$ is a zero-energy ground state of any interaction with non-negative pseudopotentials such that $V_n = 0$ for all $n \geq m$; it is the highest-density ground state if all the V_n with odd $n < m$ are non-zero.

For a power-law interaction $V(\mathbf{r}) = \frac{U}{(r/l_B)^p}$, where U is the interaction energy scale,

$$V_m = \begin{cases} \frac{\Gamma(m+1-\frac{p}{2})}{m!2^p} U & \text{if } p < 2(m+1) \\ \infty & \text{otherwise.} \end{cases} \quad (17)$$

The m^{th} Haldane pseudopotential V_m is infinite when $p \geq 2(m+1)$, and diverges logarithmically as $p \rightarrow 2(m+1)$. This fact has implications for FQH states at different fillings as described below.

A. Fermionic FQHE parent states at $\nu = 1/3$ and $\nu = 1/5$

For a power-law interaction with exponent $p \geq 4$, the Haldane pseudopotential V_1 becomes divergent. The Laughlin state $|\psi_L^{(3)}\rangle$, which has coefficient $A_1 = 0$, is then the only possible antisymmetric state with finite energy at $\nu = 1/3$. Equivalently, if one normalizes the overall energy scale U such that $V_1 \equiv 1$, all the higher pseudopotentials vanish, and $|\psi_L^{(3)}\rangle$ is the only zero-energy state. This implies that, for fermions in the LLL at filling $1/3$, any power law interaction with $p \geq 4$ becomes effectively a *contact* interaction, $V(\mathbf{r}) \sim \nabla^2 \delta(\mathbf{r})$. Such an interaction does not introduce a metric ε_{ab} into the problem, and the band mass tensor m_{ab} alone sets the FQH state's geometry. In other words, the problem is isotropic up to a rescaling of the coordinates, hence the anisotropy of the bare fermions carries over completely

to the many-body ground state, giving $\alpha_{\text{QH}} = \alpha$. The linear response coefficient in particular is $c_1 = 1$.

If the interaction power-law exponent satisfies $p \geq 8$, then *both* V_1 and V_3 diverge. At $\nu = 1/3$, the Laughlin state $|\psi_L^{(3)}\rangle$ (which has $A_1 = 0$ but $A_3 \neq 0$) has a divergent energy $E \sim A_3 V_3$. However it is still the ground state, as V_1 diverges more strongly than V_3 . If one regularizes the interaction by introducing a short-distance cutoff Δ (as we shall do later to ensure numerical stability), then as $\Delta \rightarrow 0$ one has $V_m \sim \Delta^{2(m+1)-p}$, hence $V_3/V_1 \sim \Delta^4$. Therefore the divergence of V_1 is dominant and $|\psi_L^{(3)}\rangle$, being the unique state with $A_1 = 0$ at $\nu = 1/3$, remains the ground state. For $\nu = 1/5$ instead the divergence of V_3 has an important effect: the Laughlin state $|\psi_L^{(5)}\rangle$ (with $A_1 = A_3 = 0$) becomes the unique finite-energy ground state, with the attendant conclusions about the transference of anisotropy.

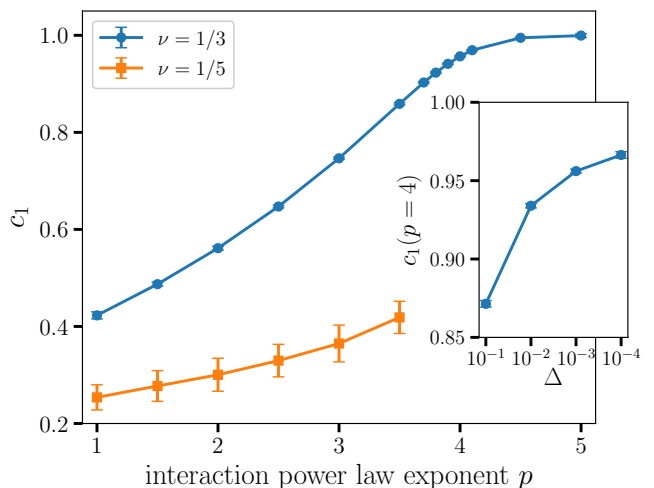


FIG. 1. The linear coefficient c_1 of the response of the $\nu = 1/3$ and $\nu = 1/5$ FQH states to anisotropy is plotted as a function of interaction power-law exponent p . Simulations are carried out for 5 different sizes L_y and bond dimensions $\chi = 2048$ to 4096 to account for finite size and truncation effects. We estimate errors from the standard deviation of the three best converged sizes at the highest bond dimension. The short length-scale cut-off Δ is fixed at 10^{-3} . (Inset) The value of c_1 at the critical power law $p_c = 4$ for $\nu = 1/3$ is plotted as a function of the cutoff Δ . It appears to flow to the theoretical value of 1 as $\Delta \rightarrow 0$.

It is straightforward to see how this generalizes to different fractions: for filling $\nu = 1/m$, there is a critical power law $p_c(m) = 2(m-1)$ above which $\alpha_{\text{QH}} = \alpha$ and thus $c_1 \equiv 1$. For $p < p_c(m)$, we instead expect the anisotropy of the bare fermions to carry over only incompletely to the quantum Hall state, giving $c_1 < 1$.

This picture implies a non-analytical behavior of c_1 as the interaction is made shorter ranged: $c_1(p)$ cannot be analytical at $p = p_c$, as $c_1(p > p_c) \equiv 1$ while $c_1(p < p_c)$ is a nontrivial smooth function. This may manifest as a kink (a discontinuity in the first deriva-

tive), a discontinuity in higher derivatives, or a more subtle non-analytical feature. For comparison, in the case of Gaussian interaction $V(r) = e^{-r^2/2s^2l_B^2}$ (see Eq. (14)), we have $c_1 = (1 + s^2)^{-1}$. This is a smooth function of s that flows asymptotically towards 1, in a *filling-independent* manner, as the range is made shorter ($s \rightarrow 0$).

We numerically compute the anisotropy for a modified power-law interaction

$$V(r) = \frac{l_B}{r} \left(\frac{r^2}{l_B^2} + \Delta^2 \right)^{\frac{1-p}{2}}, \quad (18)$$

where Δ is a small regularizing parameter needed to ensure numerical stability at short length scales. In the limit $\Delta \rightarrow 0$, we recover the familiar power-law with exponent p . For Coulomb interaction ($p = 1$), it was found²⁹ that $c_1 \approx 0.43$. The result of our numerical fit (Fig. 1) for the linear anisotropy coefficient c_1 is consistent with c_1 increasing monotonically with the power-law exponent p for $p < 4$, and attaining a constant value $c_1 = 1$ for $p \geq 4$. The deviation from the theoretical prediction near $p = 4$ is entirely due to our use of a short range numerical cut-off Δ . As we reduce Δ , the numerically obtained c_1 converges to the expected value. As the singularity at $p = 4$ is logarithmic, we must span several orders of magnitude in Δ to observe a significant drift of the result. The approach to $\Delta \rightarrow 0$ is ultimately limited by numerical instability. For the $\nu = 1/5$ FQH state, the value of c_1 is smaller than that for $\nu = 1/3$ at every power-law considered, indicating that the transference of anisotropy is much less in this case. The value of c_1 also increases much more slowly as a function of power-law exponent, and is consistent with reaching a value of $c_1 = 1$ at $p = 8$, although numerical stability issues limit the range of our study to smaller values of p .

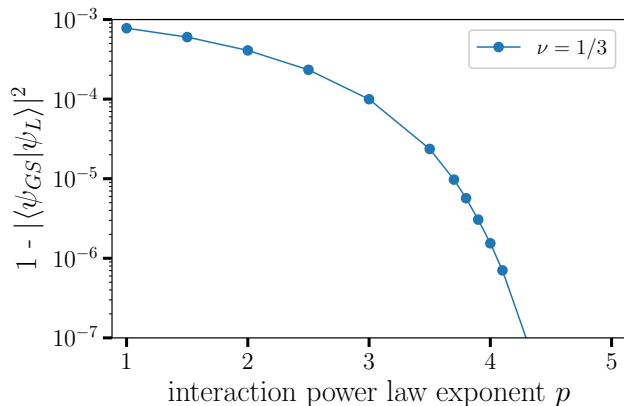


FIG. 2. The overlap (per quantum of flux) of the ground state of the power-law interaction at $\nu = 1/3$ with that of the Laughlin wavefunction $|\psi_L^{(3)}\rangle$ is plotted as a function of the power-law exponent at zero anisotropy. The system size is fixed at $L_y = 20l_B$, the cut-off $\Delta = 10^{-3}$ and bond dimension for iDMRG is $\chi = 4096$.

In Fig. 2, we show the overlap (per flux quantum) of the

ground state of the power-law interaction, as obtained by the iDMRG algorithm, with that of the Laughlin wavefunction, obtained for a V_1 Haldane pseudopotential interaction. The overlap is already very high ($> 99.9\%$) for Coulomb interaction – a fact that contributed to the initial success of Laughlin’s *ansatz* as a description of the FQH effect. However, as the power-law is made shorter ranged by increasing p , the overlap increases further and rapidly approaches 1 as $p \rightarrow 4$, in agreement with the theoretical arguments made above, and in a manner compatible with the response to anisotropy plotted in Fig. 1.

B. Fermionic FQHE daughter state at $\nu = 2/5$

Many different FQH fractions $\nu \neq 1/m$ have been explained by the hierarchy⁸ or composite fermion (CF)^{9,67} pictures. These can inform our expectation of the response of these states to anisotropy, and we briefly review them in the following.

In the hierarchy picture, introducing a number $N_{qh} = (N_e + 1)/2p$ of quasiholes or quasielectrons into the Laughlin state at a parent filling $\nu = 1/q$ creates a daughter state of quasiparticles at electronic filling $\frac{2p}{2pq \pm 1}$. This daughter state is described by a Laughlin wavefunction $|\psi_L^{(q)}\rangle$ of quasiparticles. Starting with any daughter state, the process can be recursed to obtain a whole tree of states originating from a single parent. The hierarchy states are FQH liquids provided the pseudopotentials for quasiparticles decay sufficiently quickly and the energy gaps are large enough. Since the wavefunctions of daughter states are related to those of the parent states, we would expect the response to anisotropy to follow similarly.

In the CF picture, one starts from the concept of flux attachment: $2p$ quanta of magnetic flux are attached to each electron so that the resulting object, the composite fermion, sees an effective filling $\nu_{CF} = \frac{\nu}{1-2p\nu}$. Then the integer quantum Hall effect of CFs, $\nu_{CF} = n \in \mathbb{Z}$, explains electronic fractions $\frac{n}{1+2pn}$. The original Laughlin state corresponds to $n = 1$, while other integers form a “Jain sequence” that culminates in the even-denominator CFL state $\nu = \frac{1}{2p}$. In this picture, since the entire Jain sequence is ultimately created from the same object, it is natural to associate a shape to the CF and expect it to be inherited by all fractions in the sequence.

In Fig. 3, we plot the numerical fit to linear anisotropy coefficient c_1 at filling $\nu = 2/5$. This state is a daughter of the $\nu = 1/3$ state, and based on the previous discussion we expect it to show a similar response as its parent state. In line with our expectations, we see quantitative similarities over the entire range of interaction with the plot of c_1 for the $\nu = 1/3$ state in Fig. 1. In particular we again see a critical power law exponent $p_c = 4$ above which the anisotropy is transferred completely to the FQH state.

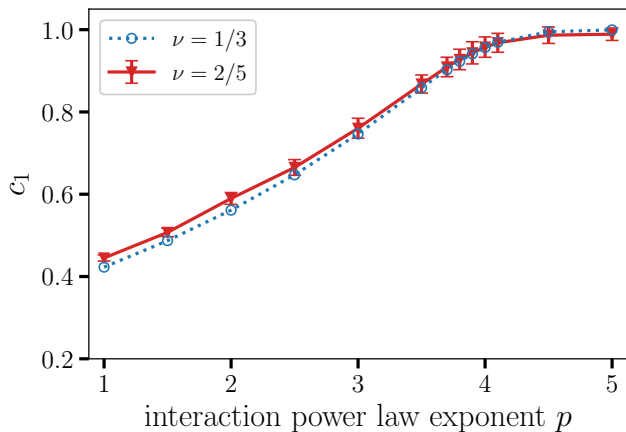


FIG. 3. The linear anisotropy coefficient c_1 for the FQH state at filling $\nu = 2/5$. The short-distance cut-off is fixed at $\Delta = 10^{-3}$. For comparison, the curve from Fig. 1 for $\nu = 1/3$ is plotted as a dashed blue line.

C. Composite Fermi liquid state at $\nu = 1/2$

In Ref.²³, the transference of anisotropy to the CFL for Coulomb ($1/r$) and dipolar ($1/r^3$) interactions was studied. The coefficient c_1 for the two cases was found to be $\simeq 0.49$ and $\simeq 0.80$. Here, we perform calculations for the intermediate case $V(r) = 1/r^2$, using system sizes $13l_B \leq L_y \leq 24l_B$ and bond dimension $\chi = 4096$. Following the method outlined in Sec. II, we find a coefficient $c_1 \simeq 0.61$ (Fig. 4). Unlike the gapped FQH case, here each point is calculated by aggregating data over all sizes, which makes it impossible to characterize the error from the variation of c_1 with system size. We instead estimate the uncertainty to be approximately 0.02, based on the extremes of acceptable fits to the elliptical Fermi surface.

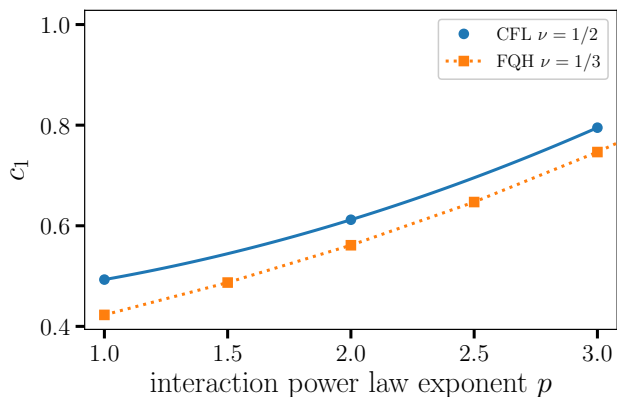


FIG. 4. The linear anisotropy coefficient c_1 for the $\nu = 1/2$ CFL, for three different power laws. For comparison, the curve from Fig. 1 for $\nu = 1/3$ is also plotted.

This result is consistent with our understanding that the transference of anisotropy to the CFL becomes larger as the power-law exponent p increases. It is also interesting that the c_1 coefficient extracted for the CFL is consistently larger than that for the $\nu = 1/3$ FQH state and its daughter state $\nu = 2/5$: the discrepancy is small, especially considering the difficulty of analyzing finite-size effects on the CFL results, but it is nonetheless reproduced systematically, for three distinct power laws, with similar magnitude. The hierarchy sequence starting from the $\nu = 1/3$ FQH state culminates in the CFL at $\nu = 1/2$. It is an interesting open question whether the response to anisotropy of gapped FQH states in the sequence drifts smoothly towards the CFL value as ν is increased, or whether the response changes discontinuously as the gap closes. The small discrepancy between $\nu = 2/5$ and $\nu = 1/3$ seen in Fig. 3 seems to support the former scenario; however, more work is needed to settle this issue.

IV. BOSONIC STATES

The FQH can also be realized in systems of bosons with a repulsive interaction in an external magnetic field. In this section, we repeat the analysis of fermionic FQH states of Sec. III on the analogous states for bosonic systems. Our results, including the singularity at power law exponent $p_c(m) = 2(m - 1)$ and the identical response of parent and daughter states, should apply regardless of statistics of the underlying constituents. Bosonic FQH states are therefore a natural testbed for our results.

The projected LLL Hamiltonian remains the same as in Eq. (3). In this case, the ground state at filling fractions $\nu = 1/m$ is a gapped incompressible liquid for *even* m . The ground state energy E_{gs} depends only the even pseudopotentials V_{2m} . The bosonic Laughlin wavefunction at filling $\nu = 1/m$ with even m is the exact, zero-energy, maximum density ground state of a potential whose only non-zero Haldane pseudopotentials are V_{2k} , $k < m/2$. A gapped FQH phase, adiabatically connected to the Laughlin state, is stable when higher pseudopotentials V_2, V_4, \dots are turned on^{68,69}, as is the case for Coulomb interactions.

The same argument we formulated for anisotropy of fermions applies to bosons as well: any power law $V(r) \sim r^{-p}$ with $p \geq 2(m - 1)$ maps onto a contact interaction and gives $c_1 = 1$, whereas lower powers may give non-trivial response $0 < c_1 < 1$.

Below we investigate the effects of anisotropy on bosonic FQH states at $\nu = 1/2, 1/4$ and $2/3$.

For the bosonic FQH state at $\nu = 1/2$, with Coulomb interaction, we expect the transference of anisotropy to be partial, with $c_1 < 1$, since the critical power law $p_c = 2$. For $\nu = 1/4$, the critical power law $p_c = 6$.

In Fig. 5, we see that the linear anisotropy coefficient $c_1 \approx 0.69$ for Coulomb interactions at $\nu = 1/2$, and rises monotonically with p . There is a kink at $p = 2$, which is

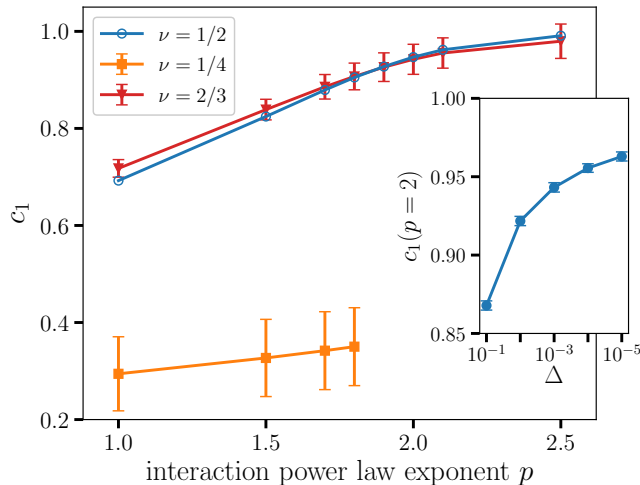


FIG. 5. Similar to Fig. 1, but for bosonic parent fractions at $\nu = 1/2$ and $\nu = 1/4$, and the bosonic daughter state at $\nu = 2/3$. The variation of linear anisotropy coefficient c_1 with power-law exponent p is plotted. For simulations, a cut-off $\Delta = 10^{-3}$ is used. Points are estimated by running simulations over 5 different sizes L_y and bond dimension $\chi = 2048$ to 4096. The inset exhibits the variation of c_1 with Δ for $p_c = 2$ for filling $\nu = 1/2$, showing the convergence of $c_1(p_c) \rightarrow 1$ in the $\Delta \rightarrow 1$ limit.

softened by our use of a short length scale cutoff Δ . For interaction power law exponent $p \geq 2$, $c_1 = 1$.

For the state at $\nu = 1/4$, the value of c_1 is smaller than that for $\nu = 1/2$. Numerical instability limits our investigations to small power laws, but nevertheless the slow growth in $c_1(p)$ is consistent with a kink in $c_1(p)$ at a much larger power-law exponent.

The bosonic FQH state at $\nu = 2/3$ is a daughter of the $\nu = 1/2$ state. The responses of both states to anisotropy are found to be very close to each other, within the numerical accuracy of our method. This result parallels the one we found for fermionic daughter states in the previous section.

V. C_4 -SYMMETRIC DISTORTIONS

In this Section we extend our discussion beyond elliptical anisotropy to consider band dispersions with discrete four-fold (C_4) rotational symmetry, which is often present in real band structures but does not seem to play as much of a role as band mass (C_2) anisotropy in shaping the FQH state. These type of distortions have recently gained attention in contexts ranging from the integer quantum Hall effect³⁴, a field-theoretic approach to the CFL⁷⁰, and the out-of-equilibrium dynamics of the FQH “graviton”³¹. Generalized anisotropic pseudopotentials²⁶ have been developed to address this and other types of distortions beyond band mass anisotropy.

Previous numerical work²⁵ has analyzed this problem

for the CFL at filling $\nu = 1/2$, where the effect of C_4 symmetric distortions was found to be substantially smaller than that of C_2 distortions (by about one order of magnitude at the level of linear response). The distortions were measured from the shape of the CFL Fermi contour via the same method outlined in Sec. III C, which probes momenta $q \approx \ell_B^{-1}$. This raises the question of long-wavelength ($q \rightarrow 0$) response in incompressible FQH states, where the quartic behavior of $S(\mathbf{q})$ may provide a natural channel for C_4 symmetric distortions and thus one may expect stronger effects.

A. Model and method

We follow the method used Ref.²⁵, which we review below. We consider the dispersion

$$\varepsilon(k, \theta) = k^4(1 + \tanh(2\gamma) \cos(4\theta)) \equiv E_F \left(\frac{k}{k_F(\theta)} \right)^4, \quad (19)$$

which is C_4 -symmetric, is a polynomial in k_x , k_y , and defines a Fermi contour $k_F(\theta)$ whose overall magnitude depends on electron density (n), but whose shape depends only on γ , not n . As a result, the zero-field Fermi surface for any electron density is characterized by a fixed anisotropy

$$\alpha \equiv \frac{k_F(\pi/4)}{k_F(0)} = e^\gamma. \quad (20)$$

From Eq. (19) we calculate the generalized LLL orbital by quantizing

$$k_x \mapsto \frac{a + a^\dagger}{\sqrt{2}l_B} \quad k_y \mapsto \frac{a - a^\dagger}{i\sqrt{2}l_B} \quad (21)$$

and numerically finding the ground state of the resulting sparse Hamiltonian. The Landau level mixing coefficients in the expansion of the ground state $|\tilde{0}\rangle$ in the basis of isotropic Landau levels $\{|N\rangle : N \geq 0\}$,

$$|\tilde{0}\rangle \equiv \sum_N u_N |N\rangle, \quad (22)$$

are such that $u_N \neq 0$ only for $N = 0, 4, 8, \dots$ because of the C_4 symmetry. These coefficients can be used to calculate the anisotropic form factor $F_{\tilde{0}\tilde{0}}(\mathbf{q})$ as a linear combination of isotropic ones, which are known analytically. The resulting interaction is then used to build the matrix product operator Hamiltonian for the iDMRG method.

In the 2D thermodynamic limit, the system has C_4 symmetry, so the guiding center structure factor of the many-body FQH ground state, $S(q)$, must be of the form

$$S(q, \theta) = e^{2D} (1 + \tanh(2\sigma) \cos(4\theta)) q^4. \quad (23)$$

D is even under C_4 , while σ and γ are odd. This directly generalizes the definitions of γ , D and σ used previously

for the case of band mass anisotropy. It remains true, in particular, that $\alpha_{\text{QH}} = e^\sigma$, if one defines α_{QH} as the anisotropy of equal-value contours of $S(q)$ at $q \ll l_B^{-1}$, in analogy to Eq. (20). Letting

$$\lambda = \lim_{q_x \rightarrow 0} S(q_x, 0)/q_x^4, \quad (24)$$

we have

$$\sigma = \frac{1}{4} \ln \frac{\lambda(\gamma)}{\lambda(-\gamma)}, \quad D = \frac{1}{2} \ln \left(\frac{\lambda(\gamma) + \lambda(-\gamma)}{2} \right). \quad (25)$$

In the following we focus on fermionic states at fillings $\nu = 1/3$ and $1/5$ with Coulomb interaction.

B. Laughlin state, $\nu = 1/3$

For the $\nu = 1/3$ state, we obtain the results shown in Fig. 6. The functions $\sigma(\gamma)$ and $D(\gamma)$ are approximately given by

$$\sigma(\gamma) \simeq 0.11\gamma, \quad D(\gamma) \simeq -0.66 + 0.04\gamma^2, \quad (26)$$

where the cubic term in σ is found to be compatible with zero: $c_3 = 0 \pm 0.01$. The linear term in the response σ is significantly larger than what was found in the CFL²³ ($c_1 \simeq 0.06$ in this paper's notation), but still only a quarter (i.e. much smaller than) the magnitude of the response to C_2 band mass anisotropy, $c_1 \simeq 0.43$. Another striking difference with respect to the elliptical case is that the isotropic dilation, parametrized by D , is not constant. It is, on the contrary, of comparable magnitude as the distortion σ itself. The quadratic coefficient $c_2 \simeq 0.04$ is not compatible with zero, as is clear from Fig. 6.

C. Laughlin state, $\nu = 1/5$

The $\nu = 1/5$ state, as discussed in Sec. III A, has significantly weaker response than the $\nu = 1/3$ state. In Ref.²⁹ this was attributed to a general feature of flux attachment: the single-particle orbitals attached to each electron are most sensitive to anisotropy near the core, and get progressively closer to circular as one moves outwards; therefore attaching more fluxes (i.e. lowering the filling) gives rise to *less anisotropic* FQH states.

The results for $\nu = 1/5$, shown in Fig. 7, are therefore surprising. We find

$$\sigma(\gamma) \simeq 0.10\gamma + 0.08\gamma^3, \quad D(\gamma) \simeq -0.24 + 0.05\gamma^2. \quad (27)$$

The magnitude of the response σ is *not* smaller than that of the $\nu = 1/3$ state: the linear coefficients c_1 are compatible within finite-size uncertainty, while the cubic coefficient c_3 is significantly larger in this case. We also find that the isotropic rescaling D , despite much stronger finite-size effects, appears to be consistent with

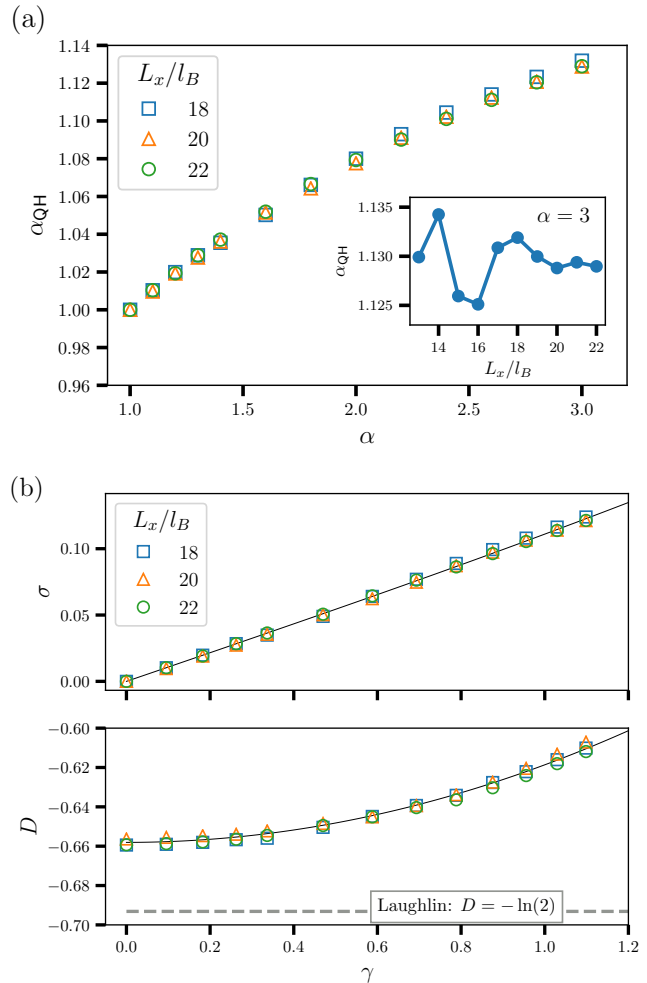


FIG. 6. Numerical results for $\nu = 1/3$ with Coulomb interaction, obtained with DMRG bond dimension $\chi = 1000$. (a) Anisotropy of the FQH state $\alpha_{\text{QH}} = e^\sigma$ as a function of band anisotropy $\alpha = e^\gamma$. Inset: finite-size oscillations of α_{QH} at fixed $\alpha = 3$. (b) Logarithmic parameters σ and D as a function of γ . Finite size effects are very small. Continuous lines correspond to fits of the data at $L_x = 21l_B$ to fixed-parity polynomials of the form $\sigma = c_1\gamma + c_3\gamma^3$ and $D = c_0 + c_2\gamma^2$. Results for data averaged over all sizes are similar. The dashed line shows the lower bound $D \geq -\frac{1}{2} \ln(2)$, achieved by the Laughlin state $|\psi_L^{(3)}\rangle$ (with pure V_1 interaction), for comparison.

that of the $\nu = 1/3$ state, up to an expected shift in the constant term: for the Laughlin state $|\psi_L^{(m)}\rangle$ one has $D(0) = \frac{1}{2} \ln \frac{m-1}{8}$; this value sets a lower bound for realistic interactions, e.g. Coulomb⁷¹, hence the offset in going from $m = 3$ to $m = 5$.

The response σ in Eq. (27) is remarkable because it also signals a qualitatively distinct behavior of the $\nu = 1/5$ state. For $\nu = 1/3$, the anisotropy α_{QH} is found to be a concave function of α (close to $\alpha_{\text{QH}} = \alpha^{0.11}$), which may be related to the apparent saturation of composite fermion anisotropy α_{CF} observed in Ref.²⁵. On the con-

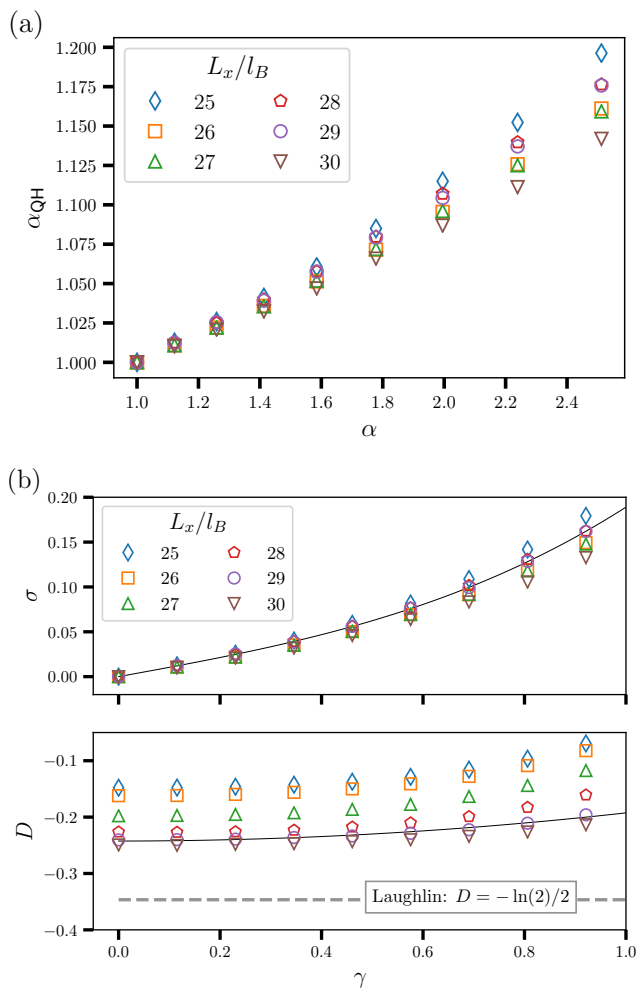


FIG. 7. Numerical results for $\nu = 1/5$ with Coulomb interactions, obtained with DMRG bond dimension $\chi = 2000$. (a) Anisotropy of the FQH state $\alpha_{\text{QH}} = e^\sigma$ as a function of band anisotropy $\alpha = e^\gamma$. (b) Logarithmic parameters σ and D as a function of γ . Finite size effects are stronger in this case, despite the larger sizes considered (up to $L_x = 30l_B$). Continuous lines correspond to fits of the data at $L_x = 29l_B$ to the same polynomial forms as in Fig. 6. The drift of D with size must stop before saturating the lower bound $D \geq -\ln(2)$ attained by $|\psi_L^{(5)}\rangle$.

trary, for $\nu = 1/5$ we find that α_{QH} is a *convex* function of α , growing super-linearly in the interval $1 \leq \alpha \lesssim 3$ that we investigated numerically, and suggesting that much stronger distortions may be possible at larger α .

This overall stronger response is in striking contrast to the results for band mass anisotropy and their interpretation given in Ref. 29. Secondly, the isotropic rescaling D , despite much stronger finite-size effects, appears to be consistent with that of the $\nu = 1/3$ state, up to an expected shift in the constant term. Since the Laughlin state $|\psi_L^{(m)}\rangle$ has $D(0) = \frac{1}{2} \ln \frac{m-1}{8}$, in going from $m = 3$ to $m = 5$ one expects a shift of $\frac{1}{2} \ln 2 \approx 0.34$ even for Coulomb interaction.

This counterintuitive result may be a special feature of the $\nu = 1/5$ state. At filling $\nu = 1/m$, one can write a deformed Laughlin wavefunction with exact C_{m-1} symmetry as follows³⁵:

$$\Psi_m(\{z\}) = e^{-\frac{1}{4} \sum_i |z_i|^2} \prod_{i < j} (z_i - z_j) \times \prod_{\mu=0}^{m-1} (z_i - z_j - \eta e^{2\pi i \mu / m}), \quad (28)$$

where $\eta \equiv |\eta|e^{i\phi}$ is a parameter controlling the magnitude ($|\eta|$) and orientation (ϕ) of the distortion. In other words it is possible to split the m -fold zero into a single zero (necessary for fermionic antisymmetry) and $m-1$ zeros arranged on the vertices of a regular polygon, which has C_{m-1} discrete rotational symmetry. One can thus construct a C_4 -symmetric Laughlin-like state for $\nu = 1/5$, but not $\nu = 1/3$.

On the other hand, a C_N symmetric state can be constructed for all even $N < m$: for example, by modifying the prescription in Eq. (28) to

$$\Psi_m(\{z\}) = e^{-\frac{1}{4} \sum_i |z_i|^2} \prod_{i < j} (z_i - z_j)^{m-N} \times \prod_{\mu=1}^N (z_i - z_j + \eta e^{2\pi i \mu / N}). \quad (29)$$

This suggests that the Laughlin state $|\psi_L^{(m)}\rangle$ may have a natural way of responding to distortions with C_N symmetry for $N \leq m-1$, but *not* for larger N . This would explain the weaker response of $\nu = 1/3$ to C_4 distortions relative to $\nu = 1/5$.

Unfortunately this conjecture is hard to test beyond this level, for two reasons: (i) the difficulty in studying the next Laughlin state, $|\psi_L^{(7)}\rangle$ at $\nu = 1/7$, and (ii) the difficulty in identifying and calculating observables which can display C_6 -symmetric distortions. At filling $\nu = 1/7$ Coulomb interactions favor a Wigner crystal over the incompressible FQH state⁶, and while the Laughlin state can be engineered numerically for suitably short-ranged interactions, finite-size effects are bound to be much worse than for the $\nu = 1/3$ and $1/5$ states. As for signatures of C_6 -symmetric anisotropy, any anisotropic terms in $S(q)$ at small q would occur at $\mathcal{O}(q^6)$ and would thus be drowned out by the leading isotropic term q^4 . One would need to identify higher-order correlators with a leading q^6 behavior, which would also be considerably harder to calculate numerically.

These issues, while interesting and still largely unexplored, go beyond the scope of the present work and we leave them to future investigations.

VI. DISCUSSION

We have systematically studied the response of fractional quantum Hall states to geometric distortions for

a wide variety of interaction potentials and LLL filling fractions, for both fermionic and bosonic particles. We considered isotropic interactions and introduced anisotropy by means of the single-particle dispersion. The anisotropy of the FQH ground state then results from a competition between the shape of interactions and that of single-particle orbitals.

We have performed infinite density matrix renormalization group (iDMRG) simulations of the problem and extracted the anisotropy of the FQH ground state from its static guiding center structure factor, in particular, from its long-wavelength limit. This approach relies on the ability to accurately probe very long wavelength in one direction, which is a unique strength of the infinite DMRG method.

Generically, for power-law interactions $V(r) \sim r^{-p}$, we found confirmation to the intuition that larger values of p correspond to “shorter-range” interactions and thus are less effective at washing out the anisotropy of single-particle orbitals. Even though all power law interactions are strictly speaking long-range, we make the above intuition more rigorous by considering their pseudopotential decomposition. Doing so reveals singularities at special values of the power law exponent p , beyond which interactions effectively transition from long range to contact. When this happens, only one geometry is left in the problem, and the FQH fluid simply inherits the same anisotropy as the single-particle orbitals.

In particular, we found that for filling $1/m$ (with m even for fermions and odd for bosons) this transition occurs at $p = 2(m - 1)$. This has several interesting implications. For one, it supports the idea, presented in Ref.²⁹, that Laughlin states in the presence of band mass anisotropy should get *less anisotropic* with decreasing filling. Bosonic $\nu = 1/2$ achieves maximal anisotropy at $p = 2$, followed by fermionic $\nu = 1/3$ at $p = 4$, etc; low-filling states thus achieve maximal anisotropy only for very large p . Combined with our numerical data for $1 \leq p \lesssim 4$, this strongly suggests that the transference of anisotropy to this type of FQH states is monotonically decreasing with m for generic interactions.

One more consequence of these results is the prediction that certain FQH states with particular kinds of interactions should have a trivial geometric degree of freedom; i.e., that their intrinsic metric should be completely decided by single-particle physics. This conclusion applies whenever $p > 2(m - 1)$, which applies, in particular, to the bosonic $\nu = 1/2$ state with dipolar ($p = 3$) interaction. Interestingly, this state could be realized using ultracold polar molecules in an optical lattice with synthetic gauge potentials⁵².

We also find that “daughter states” derived from the Laughlin states via the hierarchy or composite fermion pictures show the same response to band mass anisotropy as their parent state, supporting the idea that parent and daughter states alike are ultimately created from the same anisotropic object. This was already observed for Coulomb interactions, but here we find the same re-

sult across a range of power law interactions, supporting the universality of this conclusion. Intriguingly, the non-analyticity at $p = 2(m - 1)$ is found in the daughter states as well as the parent states. This does not follow trivially from the pseudopotential decomposition.

One question that remains open is that of the relationship between the $\nu = 1/2$ fermionic CFL and the Jain sequence that emanates from it and culminates at $\nu = 1/3$. Being made of the same composite fermion building blocks, we would expect the fermionic $\nu = 1/2$ and $\nu = 1/3$ to have the same response. However, the CFL appears to have slightly stronger response to anisotropy than the $\nu = 1/3$ FQH state (though much weaker response than the bosonic $\nu = 1/2$ FQH state). This may point to a slow drift of the response along the Jain sequence, which we fail to resolve numerically; or it may be a singular feature of the gapless CFL state that sets it apart from the gapped fractions in the sequence. It is worth pointing out that the definition of anisotropy for FQH states relies on their incompressibility (the quartic behavior of $S(q)$ near $q = 0$), while for the CFL it is based on the Fermi contour, at $q \approx \ell_B^{-1}$; the small discrepancy could be a consequence of this different definition also. Finally, it may also arise from finite-size effects, which are better controlled in gapped FQH states than they are in the CFL. Consequently, the nature and explanation of this discrepancy remains an open issue.

Finally, we have extended our investigation to band distortions with discrete four-fold (C_4) rotational symmetry. There we have found surprisingly that trend of decreasing anisotropy with decreasing filling is inverted, at least in going from $\nu = 1/3$ to $\nu = 1/5$. We conjecture that this exception to the trend may come from the ability of Laughlin states with $\nu = 1/m$ to naturally accommodate C_N -symmetric distortions by displacing some of the zeros in their wavefunction in a pattern with the appropriate symmetry. For fermionic states, this is possible only for $N \leq m - 1$, as one zero (for each pair of electrons) is fixed by antisymmetry. In particular, for C_4 symmetry, this distortion is admissible at $\nu = 1/5$ but not at $\nu = 1/3$. Developing C_4 -symmetric distortions may thus be more energetically costly at $\nu = 1/3$; as a result the ground state may be closer to the isotropic Laughlin state. This explanation, if correct, implies that a similar result should hold for C_N -symmetric distortions at filling $\nu = 1/(N + 1)$, e.g. for C_6 and $\nu = 1/7$. However this would be rather challenging to probe numerically with the method used here, and is left as another direction for future work.

ACKNOWLEDGMENTS

The iDMRG calculations were carried out using libraries developed by Roger Mong, Michael Zaletel and the TenPy collaboration. This work was supported by DOE BES grant DE-SC0002140.

- ¹ S. Girvin and R. Prange, *The Quantum Hall Effect* (Springer-Verlag New York, 1990).
- ² D. Yoshioka, *The Quantum Hall Effect*, Vol. 133 (Springer Science & Business Media, 2002).
- ³ D. C. Tsui, H. L. Stormer, and A. C. Gossard, *Phys. Rev. Lett.* **48**, 1559 (1982).
- ⁴ R. B. Laughlin, *Phys. Rev. Lett.* **50**, 1395 (1983).
- ⁵ B. I. Halperin, P. A. Lee, and N. Read, *Phys. Rev. B* **47**, 7312 (1993).
- ⁶ P. K. Lam and S. M. Girvin, *Phys. Rev. B* **30**, 473 (1984).
- ⁷ R. Moessner and J. T. Chalker, *Phys. Rev. B* **54**, 5006 (1996).
- ⁸ F. D. M. Haldane, *Phys. Rev. Lett.* **51**, 605 (1983).
- ⁹ J. K. Jain, *Phys. Rev. Lett.* **63**, 199 (1989).
- ¹⁰ D. B. Balagurov and Y. E. Lozovik, *Phys. Rev. B* **62**, 1481 (2000).
- ¹¹ F. D. M. Haldane, *Phys. Rev. Lett.* **107**, 116801 (2011).
- ¹² R.-Z. Qiu, F. D. M. Haldane, X. Wan, K. Yang, and S. Yi, *Phys. Rev. B* **85**, 115308 (2012).
- ¹³ B. Yang, Z. Papić, E. H. Rezayi, R. N. Bhatt, and F. D. M. Haldane, *Phys. Rev. B* **85**, 165318 (2012).
- ¹⁴ H. Wang, R. Narayanan, X. Wan, and F. Zhang, *Phys. Rev. B* **86**, 035122 (2012).
- ¹⁵ J. Maciejko, B. Hsu, S. A. Kivelson, Y. J. Park, and S. L. Sondhi, *Phys. Rev. B* **88**, 125137 (2013).
- ¹⁶ Z. Papić, *Phys. Rev. B* **87**, 245315 (2013).
- ¹⁷ Y. You, G. Y. Cho, and E. Fradkin, *Phys. Rev. X* **4**, 041050 (2014).
- ¹⁸ A. C. Balram and J. K. Jain, *Phys. Rev. B* **93**, 075121 (2016).
- ¹⁹ S. Johri, Z. Papić, P. Schmitteckert, R. N. Bhatt, and F. D. M. Haldane, *New Journal of Physics* **18**, 025011 (2016).
- ²⁰ O. Ciftja, *AIP Advances* **7**, 055804 (2017).
- ²¹ A. Gromov and D. T. Son, *Phys. Rev. X* **7**, 041032 (2017).
- ²² A. Gromov, S. D. Geraedts, and B. Bradlyn, *Phys. Rev. Lett.* **119**, 146602 (2017).
- ²³ M. Ippoliti, S. D. Geraedts, and R. N. Bhatt, *Phys. Rev. B* **95**, 201104(R) (2017).
- ²⁴ M. Ippoliti, S. D. Geraedts, and R. N. Bhatt, *Phys. Rev. B* **96**, 045145 (2017).
- ²⁵ M. Ippoliti, S. D. Geraedts, and R. N. Bhatt, *Phys. Rev. B* **96**, 115151 (2017).
- ²⁶ B. Yang, Z.-X. Hu, C. H. Lee, and Z. Papić, *Phys. Rev. Lett.* **118**, 146403 (2017).
- ²⁷ B. Yang, C. H. Lee, C. Zhang, and Z.-X. Hu, *Phys. Rev. B* **96**, 195140 (2017).
- ²⁸ Z. Zhu, I. Sodemann, D. N. Sheng, and L. Fu, *Phys. Rev. B* **95**, 201116(R) (2017).
- ²⁹ M. Ippoliti, R. N. Bhatt, and F. D. M. Haldane, *Phys. Rev. B* **98**, 085101 (2018).
- ³⁰ K. Lee, J. Shao, E.-A. Kim, F. D. M. Haldane, and E. H. Rezayi, *Phys. Rev. Lett.* **121**, 147601 (2018).
- ³¹ Z. Liu, A. Gromov, and Z. Papić, *Phys. Rev. B* **98**, 155140 (2018).
- ³² Z. Zhu, D. N. Sheng, L. Fu, and I. Sodemann, *Phys. Rev. B* **98**, 155104 (2018).
- ³³ K. Yang, *Phys. Rev. B* **93**, 161302(R) (2016).
- ³⁴ F. D. M. Haldane and Y. Shen, *arXiv preprint arXiv:1512.04502* (2015).
- ³⁵ O. Ciftja, C. M. Lapilli, and C. Wexler, *Phys. Rev. B* **69**, 125320 (2004).
- ³⁶ T. Gokmen, M. Padmanabhan, and M. Shayegan, *Nature Physics* **6**, 621 (2010).
- ³⁷ D. Kamburov, Y. Liu, M. Shayegan, L. N. Pfeiffer, K. W. West, and K. W. Baldwin, *Phys. Rev. Lett.* **110**, 206801 (2013).
- ³⁸ D. Kamburov, M. A. Mueed, M. Shayegan, L. N. Pfeiffer, K. W. West, K. W. Baldwin, J. J. D. Lee, and R. Winkler, *Phys. Rev. B* **89**, 085304 (2014).
- ³⁹ M. A. Mueed, D. Kamburov, Y. Liu, M. Shayegan, L. N. Pfeiffer, K. W. West, K. W. Baldwin, and R. Winkler, *Phys. Rev. Lett.* **114**, 176805 (2015).
- ⁴⁰ I. Jo, K. A. V. Rosales, M. A. Mueed, L. N. Pfeiffer, K. W. West, K. W. Baldwin, R. Winkler, M. Padmanabhan, and M. Shayegan, *Phys. Rev. Lett.* **119**, 016402 (2017).
- ⁴¹ I. Jo, M. A. Mueed, L. N. Pfeiffer, K. W. West, K. W. Baldwin, R. Winkler, M. Padmanabhan, and M. Shayegan, *Applied Physics Letters* **110**, 252103 (2017).
- ⁴² R. G. Clark, J. R. Mallett, S. R. Haynes, J. J. Harris, and C. T. Foxon, *Phys. Rev. Lett.* **60**, 1747 (1988).
- ⁴³ I. V. Kukushkin, N. J. Pulsford, K. von Klitzing, K. Ploog, R. J. Haug, S. Koch, and V. B. Timofeev, *Europhysics Letters (EPL)* **18**, 63 (1992).
- ⁴⁴ A. Pinczuk, B. S. Dennis, L. N. Pfeiffer, and K. West, *Phys. Rev. Lett.* **70**, 3983 (1993).
- ⁴⁵ L. Saminadayar, D. C. Glattli, Y. Jin, and B. Etienne, *Phys. Rev. Lett.* **79**, 2526 (1997).
- ⁴⁶ K. I. Bolotin, F. Ghahari, M. D. Shulman, H. L. Stormer, and P. Kim, *Nature* **462**, 196 (2009).
- ⁴⁷ C. R. Dean, A. F. Young, P. Cadden-Zimansky, L. Wang, H. Ren, K. Watanabe, T. Taniguchi, P. Kim, J. Hone, and K. L. Shepard, *Nature Physics* **7**, 693 (2011).
- ⁴⁸ B. E. Feldman, B. Krauss, J. H. Smet, and A. Yacoby, *Science* **337**, 1196 (2012).
- ⁴⁹ F. Amet, A. J. Bestwick, J. R. Williams, L. Balicas, K. Watanabe, T. Taniguchi, and D. Goldhaber-Gordon, *Nature Communications* **6**, 5838 (2015).
- ⁵⁰ N. Regnault and T. Jolicoeur, *Phys. Rev. Lett.* **91**, 030402 (2003).
- ⁵¹ N. R. Cooper and J. Dalibard, *Phys. Rev. Lett.* **110**, 185301 (2013).
- ⁵² N. Y. Yao, A. V. Gorshkov, C. R. Laumann, A. M. Läuchli, J. Ye, and M. D. Lukin, *Phys. Rev. Lett.* **110**, 185302 (2013).
- ⁵³ N. Schine, A. Ryou, A. Gromov, A. Sommer, and J. Simon, *Nature* **534**, 671 (2016).
- ⁵⁴ N. Schine, M. Chalupnik, T. Can, A. Gromov, and J. Simon, *Nature* **565**, 173 (2019).
- ⁵⁵ M. Mulligan, C. Nayak, and S. Kachru, *Phys. Rev. B* **84**, 195124 (2011).
- ⁵⁶ Z.-X. Hu, Q. Li, L.-P. Yang, W.-Q. Yang, N. Jiang, R.-Z. Qiu, and B. Yang, *Phys. Rev. B* **97**, 035140 (2018).
- ⁵⁷ M. A. Mueed, M. S. Hossain, L. N. Pfeiffer, K. W. West, K. W. Baldwin, and M. Shayegan, *Phys. Rev. Lett.* **117**, 076803 (2016).
- ⁵⁸ Q. Shi, M. A. Zudov, J. D. Watson, G. C. Gardner, and M. J. Manfra, *Phys. Rev. B* **93**, 121404(R) (2016).
- ⁵⁹ M. S. Hossain, M. K. Ma, Y. J. Chung, L. N. Pfeiffer, K. W. West, K. W. Baldwin, and M. Shayegan, *Phys. Rev. Lett.* **121**, 256601 (2018).

- ⁶⁰ L. Du, U. Wurstbauer, K. W. West, L. N. Pfeiffer, S. Falahi, G. C. Gardner, M. J. Manfra, and A. Pinczuk, *Science Advances* **5** (2019), [10.1126/sciadv.aav3407](https://doi.org/10.1126/sciadv.aav3407).
- ⁶¹ M. P. Zaletel, R. S. K. Mong, and F. Pollmann, *Phys. Rev. Lett.* **110**, 236801 (2013).
- ⁶² M. P. Zaletel, R. S. K. Mong, F. Pollmann, and E. H. Rezayi, *Phys. Rev. B* **91**, 045115 (2015).
- ⁶³ S. M. Girvin, A. H. MacDonald, and P. M. Platzman, *Phys. Rev. Lett.* **54**, 581 (1985).
- ⁶⁴ S. M. Girvin, A. H. MacDonald, and P. M. Platzman, *Phys. Rev. B* **33**, 2481 (1986).
- ⁶⁵ S. D. Geraedts, M. P. Zaletel, R. S. K. Mong, M. A. Metlitski, A. Vishwanath, and O. I. Motrunich, *Science* **352**, 197 (2016).
- ⁶⁶ K. Yang, *Phys. Rev. B* **88**, 241105(R) (2013).
- ⁶⁷ J. K. Jain, *Composite Fermions* (Cambridge University Press, 2007).
- ⁶⁸ Y.-F. Wang, Z.-C. Gu, C.-D. Gong, and D. N. Sheng, *Phys. Rev. Lett.* **107**, 146803 (2011).
- ⁶⁹ T. Graß, P. Bienias, M. J. Gullans, R. Lundgren, J. Maciejko, and A. V. Gorshkov, *Phys. Rev. Lett.* **121**, 253403 (2018).
- ⁷⁰ D. X. Nguyen, A. Gromov, and D. T. Son, *Phys. Rev. B* **97**, 195103 (2018).
- ⁷¹ F. D. M. Haldane, *arXiv preprint arXiv:0906.1854* (2009).